International Journal of New Technology and Research (IJNTR)
ISSN:2454-4116, Volume-2, Issue-8, August 2016 Pages 43-52

Numerical Analysis of Sand Behavior based on Modified Multi-laminate Model

Farzad Peyman, Seyed Amirodin Sadrnejad

***Abstract*— Generalized form of multi-laminate integration framework satisfying compatibility of strain/deformation and equilibrium of stress/forces at each material point was employed to sum up the plastic modulus matrices of integrated planes to build up the main modulus matrix. This has been conducted through defining on plane modulus behaviors for normal, tangent and their interactions for loading and unloading. This modulus formulation enables the analysis to include the role of some material behavior aspects in the overall internal plasticity mechanism flexibility for a more accurate description of mechanism behavior under any arbitrary loading conditions. Specification of stress/strain history on the sample planes in materials with the models developed using stress/strain invariants is not feasible. This is mainly because stress/strain invariants are quantities not capable of carrying directional information with themselves.**

In this article, a constitutive model capable of predicting sand behavior under static and dynamic loading working with stress and strain invariants was modified and implemented in the multi-laminate framework to be capable of predicting any arbitrary stress path may take place on a sand element in soil structure. The proposed model is capable of presenting different stress/strain histories on the sample planes followed the applied load/deformation paths in soil materials. Model verification under different loading/unloading/reloading stress/strain paths has been examined and failure direction of sand samples was visualized upon the activities of on plane plastic strain values and then exceeding a certain limit, specified as failed plane. This constitutive model can be used to predict the sand behavior upon inherent/induced anisotropy, rotation of principal stress/strain axes, localization of stress/strain and even failure mechanism.

***Index Terms*— Multi-laminate, Modulus matrix, material behavior, constitutive law.**

I. INTRODUCTION

Multi-laminate is referred to a plane in materials with different orientation which is used for estimation of the multi-structure behavior of materials. The first idea of this model was proposed by Taylor (1938) (called slip planes). Taylor's idea was formulated in detail by Batdorf and Budiansky (1949). Many other researchers have modified this method for metals, soils and rocks.

Before 1984, the mesoscopic models were developed based on the static constraint formulation. In this approach, first the macro-stress tensor is projected on the multi-laminates. Then by introducing on-plane constitutive laws, the multi-strain vectors are defined. Finally the macro-strain tensor is obtained by using simple superposition of all the multi-strain vectors. So, with some original thinking about this method, it can be easily recognized that nevertheless the equilibrium condition is established with this method in a straightforward manner through the projection of stress tensor on the multi-laminates, the prove of satisfaction of compatibility condition seems to be not yet as a simple task. This ambiguity has been removed from 1984 by application of a new method called 'kinematic constraint approach'. In this method, which first introduced by Bazant and coworkers, instead of the stress tensor, the strain tensor is projected on the multi-laminates. So, the compatibility condition is satisfied automatically. Then, after defining the multi-stress vectors by introducing on-plane constitutive relations between multi-strain and multi-stress vectors, the macro-stress tensor will be calculated from all multi-stress vectors using the principle of virtual work instead of a simple superposition rule. Consequently, in this approach also the equilibrium condition is forcedly established. The multi-laminate developed by Sadrnejad, (1992), is capable of predicting the behaviour of geo-materials, such as rock, on the basis of sliding mechanisms, elastic behaviour of intact parts and possibilities to see different plasticity models for the most possible sliding orientations. The influences of rotation of the direction of principal stress and strain axes and induced/inherent anisotropy are included in a rational way without any additional hypotheses. The spatial strength distribution at a location as an approximation of probable mobilized sliding mechanism is proposed as an ellipsoid function built up on bedding plane.

According to the proposed model, the interface asperity shapes that is identical to model based on the minimum energy level, identify the active sliding orientations, cracks, and joints. Furthermore, the sliding behavior of any predefined existing joint through the rock mass is introduced to the matrix of global mechanical behavior based on a realistic and logical way. In the next section, we present multi-laminate formulation for arbitrary on-plane relation between stress and strain. In all the multi-laminate models such as slip-planes or multi-laminate models, first the macro-stress tensor was projected on the multi-laminates and then by introducing on-plane constitutive laws, the multi-strain components were calculated and finally the macro-strain tensor was identified by superimposition of on-plane multi-strain components upon any of sampling plane transformation matrix obtained through direction cosines of sampling points on the surface of a unit sphere:

$$\int_{\Omega} f(x,y,z)d\Omega = 4\pi \sum_{p} W_p \; f(x_p, y_p, z_p) \qquad (1)$$

However, there are two main reasons for replacing the static constraint with a kinematic constraint. The first reason is based on the formation of small multi-cracks, in which static constraint causes the continuum stress to drop off without having an effect on the strain tensor. It should be notified that the average local strain tensor around the multi-cracks and the strain tensor of the macroscopic continuum are both the same.

Farzad Peyman Department of Civil Engineering, College of Engineering, Tehran Science and Research Branch, Islamic Azad University, Tehran, Iran.

Seyed Amirodin Sadrnejad *PROFF*. Dept of Civil Eng., K.N.Toosi University of Tech., Tehran, Iran.

Another reason is the instability, the static constraint causes when there is softening on multi-laminates. It means that if there is softening, the static constraint leads to instability because of this fact that the multi-laminate strains caused by a given stress are not uniquely defined by either the softening branch or the unloading branch. So, this makes it difficult or even impossible to simulate a system of multi-cracks of many orientations, developing simultaneously in the peak stress region.

Furthermore, it is worth noting that in the static constraint approach, the equilibrium of the forces in a point are satisfied automatically because of the projection of the stress tensor on the planes, but the compatibility condition of strain tensor is met only in particular cases. In other words, the multi-strain components acting on the planes may not be always as the projection of the strain tensor, because the way of the superimposition of multi-strain components which are used in the static constraint approach does not guarantee to be the same as the summation of the projections of macro-strain tensor obtained on every plane.

In all present multi-laminate models, we noticed that in each loading step and during the projection and transportation of the module matrix of each multi-laminate to the ordinary Cartesian system, some of the important features of concrete behavior were being missed. To solve this problem and to activate all components of material behavior, here, we have considered two other orthogonal planes of each basically 26 multi-laminates on the sphere in which the number of multi-laminates have been raised to 34, by omitting the repetitive ones. To show the behavior of theses extra multi-laminates, we have considered the equivalent tangential planes of them on the sphere. In the Table 2, direction cosines and weights of the new integration points on the surface of unit sphere and in Fig. 2, their position in a cubic are shown. In addition, to satisfy both of static equilibrium and compatibility conditions, we have considered a novel method as projecting the stress tensor on the multi-laminates as described earlier in this article. Then, we derived the strain tensor in terms of the stress tensor based on a well capable constitutive relation in an ordinary three-dimensional coordinate system. In the second case, the derived strain tensor was projected or transformed on the multi-laminates. So, in this stage, by comparing the components of stress and strain on the multi-laminates we must be able to define the equal semi-microscopic constitutive relations in such a way that both of the stress and strain components on each multi-laminate are as the projections of the corresponding stress and strain tensors. This situation, in fact, is the double constraint formulation in which the equilibrium of forces and compatibility of displacements in every integration points are satisfied one by one.

In order to attain to the double constraint aspect, after analogy of the projections of stress and strain tensors on the multi-laminates obtained in the manner that was explained in the previous section, it was certain that it is necessary to separate the behavior of material into two distinct parts as deviatoric and volumetric. So if we discrete the strain tensor as the volumetric and deviatoric parts firstly and then project each of them on the multi-laminates separately, we may try to obtain the deviatoric part of the modules matrix from the behaviors which are taking place on the multi-laminates and the volumetric one which is not affected by the direction characteristics and essentially is isotropic, obtained in the ordinary coordinate system and summed up to the deviatoric part at the end of each step of loading. Total deviatoric part of constitutive matrix is computed from superposition of its counterparts in turn, are calculated based on the damage occurred on each plane depending on its specific loading conditions.

On each multi-laminate at each time of loading history, there exists one specific loading situation that it may be in one of the five mentioned basic loading conditions. For every five mood, a specific damage function according to the authoritative laboratory test results available in the literature is assigned.

II. Multi-laminate Framework

The accurate behaviour of particulate materials is to be investigated through multi-mechanics. However, the multi-mechanical behaviour of granular materials is therefore inherently discontinuous and heterogeneous. The macroscopic as an overall or averaged behaviour of granular materials is determined not only how discrete grains are arranged through medium, but also by what kinds of interactions are operating among them. To investigate the multi-mechanical behaviour of granular materials, certainly, the spatial distribution of contact points and orientation of grains must be identified. In engineering point of view, the main goal is to formulate macro-behaviour of granular materials in terms of multi-quantities. However, there exist two well-known theories that explain the relation between multi-fields and macro-fields as macro-multi relations, in a consistent manner as the average field theory and the homogenization theory.

For a granular mass such as sand that supports the overall applied loads through contact friction, the overall mechanical response ideally may be described on the basis of multi-mechanical behaviour of grains interconnections. Naturally, this requires the description of overall stress, characterization of fabric, representation of kinematics, development of local rate constitutive relations and evaluation of the overall differential constitutive relations in terms of the local quantities. Multi-laminate framework (Sadrnejad, S.A., 1992) by defining the small continuum structural units as an assemblage of particles and voids that fill infinite spaces between the sampling planes, has appropriately justified the contribution of interconnection forces in overall macro-mechanics. Upon these assumptions, plastic deformations are to occur due to sliding, separation/closing of the boundaries and elastic deformations are the overall responses of structural unit bodies. Therefore, the overall deformation of any small part of the medium is composed of total elastic response and an appropriate summation of sliding, separation/closing phenomenon under the current effective normal and shear stresses on sampling planes. These assumptions adopt overall sliding, separation/closing of inter-granular points of grains included in one structural unit are summed up and contributed as the result of sliding, separation/closing surrounding boundary planes. This simply implies yielding/failure or even ill-conditioning and bifurcation response to be possible over any of the randomly oriented sampling planes. Consequently, plasticity control such as yielding should be checked at each of the planes and those of the planes that are sliding will contribute to plastic deformation. Therefore, the granular material mass has an infinite number of yield functions usually one for each of the planes in the physical space.

Figure 1 shows the arrangement of artificial polyhedron simulated by real soil grains. The created polyhedrons are roughly by 13 sliding planes, passing through each point in medium. The location of tip heads of normal to the planes defining corresponding direction cosines are shown on the surface of unit radius sphere.

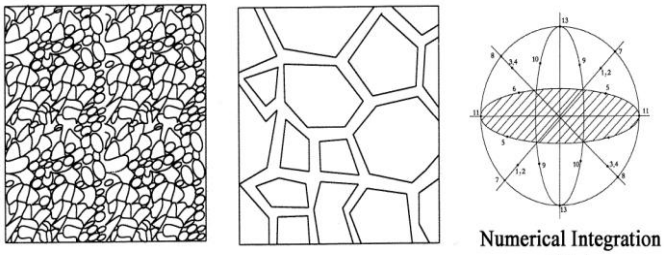

Figure 1 Soil grains, artificial polyhedrons, and sampling points, Bickley, W.G., (1941)

In ideal case, the normal integration is considered as summing up the individual multi effects correspond to infinite number of multi sampling planes. The choice of 13 planes for the solution of any three dimensional problem is a fair number.

III. Elastic-Plastic Modulus Matrices

The constitutive equations of multi-laminate model starts with the classical decomposition of strain and strain increments under the concept of elastic-plasticity in elastic and plastic parts are schematically written as follows:

$$\varepsilon = \varepsilon^e + \varepsilon^p \tag{2}$$

$$d\varepsilon = d\varepsilon^e + d\varepsilon^p \tag{3}$$

The increment of elastic strain ($d\varepsilon^e$) is related to the increments of effective stress ($d\sigma$) by:

$$d\varepsilon^e = [D^e]^{-1} d\sigma \tag{4}$$

$[D^e]^{-1}$ is elastic compliance matrix, usually assumed as linear and is obtained as follows:

$$C_{ijkl}^{-1\,e} = D_{ijkl}^{\ e} = (K - \frac{2}{3}G)\delta_{ij}\delta_{kl} + G(\delta_{ik}\delta_{jl} + \delta_{il}\delta_{jk}) \tag{5}$$

K and G are bulk and the shear modulus, respectively. Any kind of non-linearity as the change of these parameters may be applied in an incremental algorithm. For rock mass, the overall stress-strain increments relation, to obtain plastic strain increments ($d\varepsilon^p$), is expressed as:

$$d\varepsilon^p = C^p d\sigma \tag{6}$$

C^p is plastic modulusmatrix. Clearly, it is expected that all effects of plastic behaviour be included in C^p. To find out C^p, the constitutive equations for a typical slip plane must be considered in calculations. Consequently, the appropriate summation of all provided modulusmatrices corresponding to considered slip planes yields overall C^p, therefore, strain increment at each stress increment is calculated as follows:

$$d\varepsilon^p = \frac{1}{n}\sum_{i=1}^{n} W_i [L\varepsilon]^T C_i^p [L\sigma] d\sigma' \tag{7}$$

$$C_i^p = (1/H_{pi})\{\partial\psi_i/\partial\sigma\}\{\partial F_i/\partial\sigma\}^T \tag{8}$$

H_{pi} is defined as hardening modulus of i plane and is obtained as follows:

$$H_{pi} = -\{\partial F_i/\partial K_i\}^T \{\partial\psi_i/\partial K_i\} \tag{9}$$

$L\varepsilon$ and $L\sigma$ are transformation matrices for strain and stresses, respectively and n is number of planes.

A sampling plane is defined as a boundary surface that is a contacting surface between two structural units of polyhedral blocks. These structural units are parts of a heterogeneous continuum and for simplicity they are defined as a full homogeneous and isotropic material. Therefore, all heterogeneities behavior is supposed to appear in inelastic behavior of corresponding slip planes.

IV. Multi-Laminate Formulation For Strain Control

The virtual work of stress per unit volume can be written as follows:

$$\delta\dot{W} = \int_V \dot{\sigma}_{ij}\delta\varepsilon_{ij} \tag{10}$$

Furthermore, macroscopic strain vector can be resolved to normal and tangential component on each plane.

$$(d\varepsilon)_n = d\varepsilon_N + d\varepsilon_T \tag{11}$$

where:

$$(d\varepsilon_n)_j = n_k d\varepsilon_{jk} \tag{12-1}$$

$$(d\varepsilon_N)_i = n_i n_j n_k d\varepsilon_{jk} \tag{12-2}$$

$$(d\varepsilon_T)_i = (n_k\delta_{ij} - n_i n_j n_k) d\varepsilon_{jk} \tag{12-3}$$

The principle of virtual work is employed, which requires that the virtual work within a sphere of unit radius be equal to virtual work done on all planes tangential to the sphere.

$$\delta\dot{W} = \frac{4\pi}{3}\sigma_{ij}\delta\varepsilon_{ij} = 2\int_A (\dot{\sigma}_N\delta\varepsilon_N + \dot{\sigma}_T\delta\varepsilon_T)\,dA \tag{13}$$

where A is the surface of a unit hemisphere. If the constitutive relation between stress and strain is given, the following equations can be written.

$$\dot{\sigma}_N = D_{NN}^{ep}\dot{\varepsilon}_N + D_{NT}^{ep}\dot{\varepsilon}_T \tag{14-1}$$

$$\dot{\sigma}_T = D_{TN}^{ep}\dot{\varepsilon}_N + D_{TT}^{ep}\dot{\varepsilon}_T \tag{14-2}$$

Then, the equation (4) takes the form:

$$\dot{\sigma}_{ij}\delta\varepsilon_{ij} = \frac{3}{2\pi}\int_A \Big[\Big(D_{NN}^{ep}\dot{\varepsilon}_N + D_{NT}^{ep}\dot{\varepsilon}_T\Big)\delta\varepsilon_N + \Big(D_{TN}^{ep}\dot{\varepsilon}_N + D_{TT}^{ep}\dot{\varepsilon}_T\Big)\delta\varepsilon_T\Big]dA \tag{15}$$

The derivatives of the normal and tangential strain can be calculated as:

$$\frac{\partial\varepsilon_N}{\partial\varepsilon_{ij}} = n_i n_j \tag{16-1}$$

$$\frac{\partial\varepsilon_T}{\partial\varepsilon_{ij}} = \frac{n_j n_r}{\varepsilon_T}(\varepsilon_{ir} - n_i n_s \varepsilon_{rs}) \tag{16-2}$$

in which we introduce the notation:

$$A_{ij} = n_i n_j \tag{17-1}$$

$$B_{ij} = \frac{n_j n_r}{\varepsilon_T}(\varepsilon_{ir} - n_i n_s \varepsilon_{rs}) \tag{17-2}$$

Substituting equations (17-1,2) in to equation (15):

$$\sigma_{ij}\delta\varepsilon_{ij} = \frac{3}{2\pi}\int_A \Big[\Big(D_{NN}^{ep}A_{rs} + D_{NT}^{ep}B_{rs}\Big)B_{ij} + \Big(D_{TN}^{ep}A_{rs} + D_{TT}^{ep}B_{rs}\Big)B_{ij}\Big]\dot{\varepsilon}_{rs}\delta\varepsilon_{ij}\,dA \tag{18}$$

The integration in equation (18) is performed numerically by Gaussian integration using a finite number of integration points on the surface of the hemisphere. Such an integration

technique corresponds to considering a finite number of multi-laminates, one for each integration point. An approximate formula consisting of 34 integration points is proposed satisfying strain compatibility, in this study. Table 1 shows the direction cosines and weights of the integration points of 17 sampling planes (half of 34, because of existing symmetry). The orientation of the 17 planes configured in cubes for a better sense, is shown in Figure 2.

Table 1: The geometry of 17 sampling planes

Plane No	Normal Axis			w_i
	n_1	n_2	n_3	
1	$\frac{1}{\sqrt{3}}$	$\frac{1}{\sqrt{3}}$	$\frac{1}{\sqrt{3}}$	0.020277985
2	$\frac{1}{\sqrt{3}}$	$-\frac{1}{\sqrt{3}}$	$\frac{1}{\sqrt{3}}$	0.020277985
3	$-\frac{1}{\sqrt{3}}$	$\frac{1}{\sqrt{3}}$	$\frac{1}{\sqrt{3}}$	0.020277985
4	$-\frac{1}{\sqrt{3}}$	$-\frac{1}{\sqrt{3}}$	$\frac{1}{\sqrt{3}}$	0.020277985
5	$\frac{1}{\sqrt{2}}$	$\frac{1}{\sqrt{2}}$	0	0.058130468
6	$-\frac{1}{\sqrt{2}}$	$\frac{1}{\sqrt{2}}$	0	0.058130468
7	$\frac{1}{\sqrt{2}}$	0	$\frac{1}{\sqrt{2}}$	0.030091134
8	$-\frac{1}{\sqrt{2}}$	0	$\frac{1}{\sqrt{2}}$	0.030091134
9	0	$-\frac{1}{\sqrt{2}}$	$\frac{1}{\sqrt{2}}$	0.030091134
10	0	$\frac{1}{\sqrt{2}}$	$\frac{1}{\sqrt{2}}$	0.030091134
11	1	0	0	0.038296881
12	0	1	0	0.038296881
13	0	0	1	0.029390060
14	$\frac{1}{\sqrt{6}}$	$\frac{1}{\sqrt{6}}$	$\sqrt{\frac{2}{3}}$	0.019070616
15	$\frac{1}{\sqrt{6}}$	$-\frac{1}{\sqrt{6}}$	$\sqrt{\frac{2}{3}}$	0.019070616
16	$-\frac{1}{\sqrt{6}}$	$\frac{1}{\sqrt{6}}$	$\sqrt{\frac{2}{3}}$	0.019070616
17	$-\frac{1}{\sqrt{6}}$	$-\frac{1}{\sqrt{6}}$	$\sqrt{\frac{2}{3}}$	0.019070616

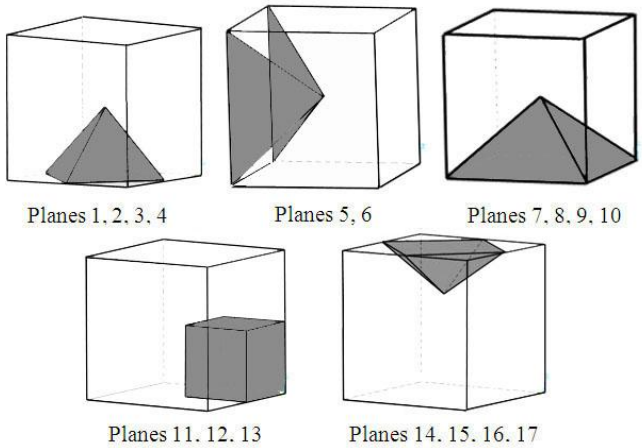

Fig. 2 Position and geometry of the multi-laminates in a cube of 17 planes.

$$\sigma_{ij} = 6\sum_{\beta=1}^{n} w_\beta \left[\left(D_{NN}^{ep} A_{rs} + D_{NT}^{ep} B_{rs} \right) p_{ij} + \left(D_{TN}^{ep} A_{rs} + D_{TT}^{ep} B_{rs} \right) B_{ij} \right]_\beta \left(\dot{\varepsilon}_{rs} \right)_\beta \quad (19)$$

$$\sigma_{ij} = 6\sum_{\beta=1}^{n} w_\beta \left(D_{ijrs}^{ep} \right)_\beta \left(\dot{\varepsilon}_{rs} \right)_\beta \quad (20)$$

In this article, the basic Pastor – Zienkiewicz[4] constitutive model was modified to work for the sliding/widening/closing of a sampling plane to be capable of seeing important behavior of sand as relation between stress and strain on multi-laminates.

V. Basic Feature Of The Developed Constitutive Model For Sand

The framework of generalized plasticity theory was first introduced by Zienkiewicz and Morz and later was extended by Pastor and Zienkiewicz [1] to model the behavior of sand under monotonic and cyclic loading as a simple model to predict the behavior of sand samples in laboratories. In generalized plasticity theory, the constitutive tensor in loading differs from constitutive tensor in unloading conditions. Using this theory, the increments of stress on any sampling plane or multi-laminates under loading and unloading condition can be written as:

$$\begin{bmatrix} d\sigma_N \\ d\sigma_T \end{bmatrix}_L = \begin{bmatrix} D_{NN}^{ep} & D_{NT}^{ep} \\ D_{TN}^{ep} & D_{TT}^{ep} \end{bmatrix}_L \begin{bmatrix} d\varepsilon_N \\ d\varepsilon_T \end{bmatrix}_L = \mathbf{D}_L^{ep} \begin{bmatrix} d\varepsilon_N \\ d\varepsilon_T \end{bmatrix}_L \quad (21)$$

$$\begin{bmatrix} d\sigma_N \\ d\sigma_T \end{bmatrix}_U = \begin{bmatrix} D_{NN}^{ep} & D_{NT}^{ep} \\ D_{TN}^{ep} & D_{TT}^{ep} \end{bmatrix}_U \begin{bmatrix} d\varepsilon_N \\ d\varepsilon_T \end{bmatrix}_U \mathbf{D}_U^{ep} \begin{bmatrix} d\varepsilon_N \\ d\varepsilon_T \end{bmatrix}_U \quad (22)$$

The subscripts ‘L’ and ‘U’ refer to loading and unloading state respectively. In fact, at each point of the stress space, a direction tensor is specified to distinguish between loading and unloading. The elasto-plastic constitutive modulus matrices can be defined as:

$$\mathbf{D}_L^{ep} = \mathbf{D}_e - \frac{\mathbf{D}_e.\mathbf{n}_{gL}.\mathbf{n}^T.\mathbf{D}_e}{H_L + \mathbf{n}^T.\mathbf{D}_e.\mathbf{n}_{gL}} \quad (23\text{-}1)$$

$$\mathbf{D}_U^{ep} = \mathbf{D}_e - \frac{\mathbf{D}_e.\mathbf{n}_{gU}.\mathbf{n}^T.\mathbf{D}_e}{H_U + \mathbf{n}^T.\mathbf{D}_e.\mathbf{n}_{gU}} \quad (23\text{-}2)$$

where H_L and H_U are the on plane plastic hardening/softening modulus in loading and unloading and $\mathbf{n}_{gL}$ and $\mathbf{n}_{gU}$ are the normal vector to plastic potential in loading and unloading conditions. The main advantage of this theory is that neither yield surface nor plastic potential surface needs to be explicitly defined. Therefore $\mathbf{n}_g$, $\mathbf{n}$ and $H_{L/U}$ can be obtained without referring to plastic potential, or yield surfaces. The normal vectors to the plastic potential and yield surfaces can be determined as follows:

$$\mathbf{n}_g^T = (n_{gN}, n_{gT}) = \left(d_g, 1\right) \Big/ \sqrt{1 + d_g^2} \quad (24)$$

$$\mathbf{n}^T = (n_N, n_T) = \left(d_f, 1\right) \Big/ \sqrt{1 + d_f^2} \quad (25)$$

where d_g can be approximated from the stress ratio $\eta = \sigma_N / \sigma_T$ as:

$$d_g = \frac{d\varepsilon_N^p}{d\varepsilon_T^p} = (1+\alpha)(M_g - \eta) \quad (26)$$

where α is a material parameter and M_g denotes the slope of critical state line. d_f is defined in a similar manner to d_g as follows:

$$d_f = (1+\alpha)(M_f - \eta) \quad (27)$$

The plastic modulus H_L for the loading condition is defined as follows:

$$H_L = H_0 \sigma_N H_f (H_v + H_s) H_{DM} \quad (28)$$

Where:

$$H_f = (1-\eta/\eta_f)^4 \quad (29)$$

$$H_s = \beta_0 \beta_1 \exp(-\beta_0 \xi) \quad (30)$$

$$H_v = (1-\eta/M_g) \quad (31)$$

$$H_{DM} = (\zeta_{\max}/\zeta)^\gamma \quad (32)$$

$$\eta_f = (1+1/\alpha) M_f \quad (33)$$

$$\zeta = \sigma_N \left[1-((1+\alpha)/\alpha)(\eta/M_g)\right]^{1/\alpha} \quad (34)$$

where H_0, β_0, β_1 and γ_U are the material parameters obtained from experiments.

The plastic modulus H_U for unloading condition is defined as follows:

$$H_U = \begin{cases} H_{U0}(M_g/\eta_U)^{\gamma_U} & \text{for } |M_g/\eta_U| > 1 \\ H_{U0} & \text{for } |M_g/\eta_U| \le 1 \end{cases} \quad (35)$$

where H_{U0} is the material parameter and η_U is the stress ratio from which unloading takes place. The vector $\mathbf{n}_{gU}$ is defined as:

$$\mathbf{n}_{gU} = (n_{gUN}, n_{gUT})^T = (-abs(n_{gN}), +n_{gT})^T \quad (36)$$

VI. Numerical Simulation

This section is concerned with various simulations of undrained behavior of Banding sand under monotonic and cyclic loading. It is worth to mentioning here that in the case of triaxial stress state, volumetric and deviatoric strain can be used instead of whole strain tensor. The relation between macro strain component and on-plane strain is as follow.

$$\begin{bmatrix} d\varepsilon_N \\ d\varepsilon_T \end{bmatrix} = \begin{bmatrix} 1/3 & 1.5(n_1^2 - 1/3) \\ 0 & 1.5 n_1 \sqrt{1-n_1^2} \end{bmatrix} \begin{bmatrix} d\varepsilon_v \\ d\varepsilon_s \end{bmatrix} \quad (37)$$

Normal strain direction is perpendicular to the multi-laminates and tangential strain direction is obtained from formula (19).

$$\mathbf{n}_{\varepsilon_T} = 1 - \frac{n_2 n_1}{\sqrt{1-n_1^2}} - \frac{n_3 n_1}{\sqrt{1-n_1^2}} \quad (38)$$

In this section, undrained behaviors of Banding sand with different relative density are simulated by proposed model. Parameters required by this model are shown in table (2). The used elastic parameters are the same as Pastor-Zienkiewicz model because only plastic strain is projected on multi-laminates. Only one value for M_f is considered during modeling. The ratio M_f/M_g seems to be proportional with relative density [1]. Increasing the value of hardening parameter with increasing relative density seems to be rational. As can be seen in Fig (3) and Fig (8), model predictions of macro behavior of undrained sand agree well with experimental results.

Figures (4), (5), (6), (7), (8) show the stress path, tangential stress vs. plastic tangential strain, normal stress vs. plastic normal strain of specimens on multi-laminates.

The value of strain in sample which has relative density %29 has reached the maximum value on multi-laminates number 14, 15, 16 and 17. This means that strain localization may be occurred on these multi-laminates. Failure mechanism of soil happened when stress state is placed on the failure line. The critical stress path is placed on the multi-laminates number 14, 15, 16 and 17. Moreover, the value of strain on the other multi planes is much smaller than multi-laminates number 14, 15, 16 and 17. This indicates that the failure plane of loose sand is placed on multi-laminates number 14, 15, 16 and 17. On the other hand, because of contractive behavior of loose sand under shear loading plastic normal strain on these multi-laminates has high value.

Table 2: Material Parameters

	D_r=29%	D_r=44%	D_r=47%	D_r=66%
k_{evo}(KPa)	35000	35000	35000	35000
G_0(KPa)	525000	525000	525000	525000
M_f	.27	.27	.27	.27
M_g	1.5	.6	.48	.44
H_0	2450	7000	12250	26250
β_0	4.2	4.2	4.2	4.2
β_1	.2	.2	.2	.2
γ	2.5	–	–	–
H_{U0}	3500000	–	–	–
γ_U	1	–	–	–

With increasing of sample density, the value of shear strain on three sets of multi-laminates becomes important. The active planes are number 1, 2, 3, 4 and 5, 6, 7, 8 and 14, 15, 16, 17. As can be seen in Fig (5) to (7), the critical first exceeding failure line are the stress paths on the multi-laminates number 14, 15, 16, 17 followed by the next set planes number 1, 2, 3, 4 and last set is planes number 5, 6, 7 and 8. This means that failure plane is placed between these multi-laminates and is closer to multi-laminates on which tangential strain has grater value. Failure plane for Fig (5) and (7) is closer to the multi-laminates number 14, 15, 16, 17 and 1, 2, 3, 4 respectively but for Fig (6), failure plane can be a certain orientation between those sets of plane. In the other words, inclination of failure plane decreases with increasing relative density of samples which was seen in experimental results [5, 6, 7, 8]. With increasing of sample density, the value of plastic normal strain on failure plane decreases. This happened because of dilative behavior of dense sand under shear loading. Cyclic behavior of Banding sand is shown in figure (8) and (9). Because of the capability of Proposed constitutive model which is capable of seeing important behavior of sand, model prediction of semi-micro behavior of undrained sand agree well with experimental results. As aforementioned before, failure plane of this sample is placed on multi-laminates number 14, 15, 16 and 17.

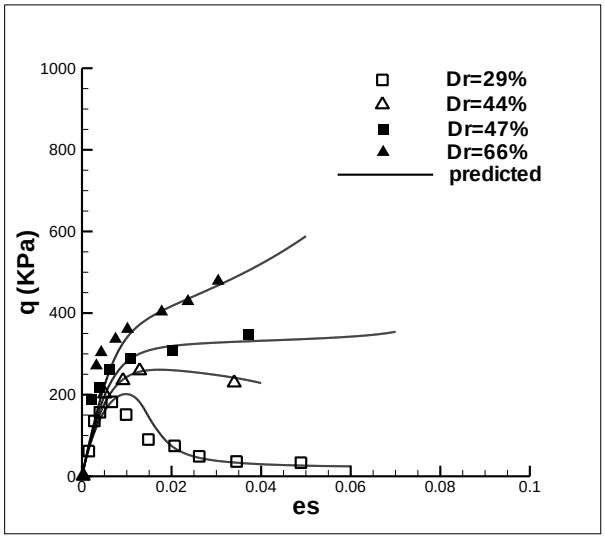

(a)

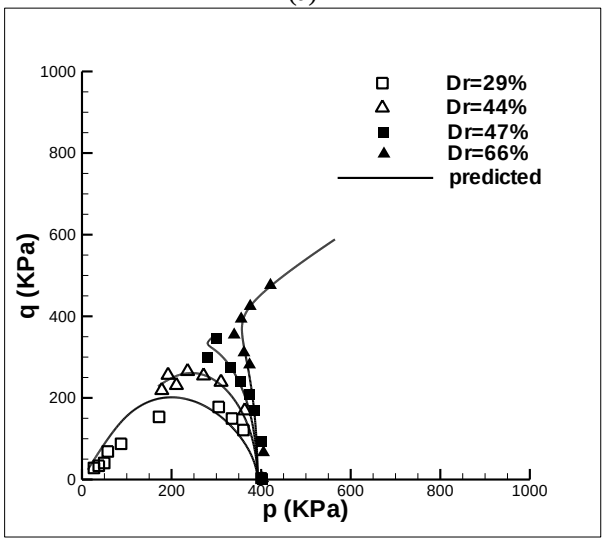

(b)

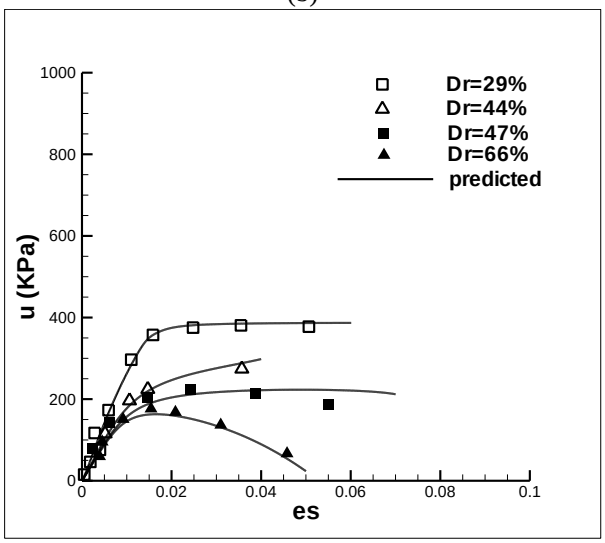

(c)

Figure (3) Undrained behavior of Banding sand a) deviatoric stress vs. shear strain b)stress path, c) pore pressure vs. shear strain under monotonic loading (Computed results shown by solid line)[4].

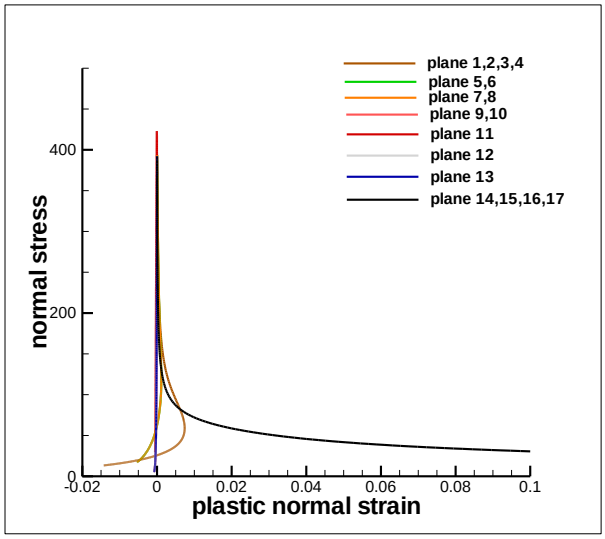

(a)

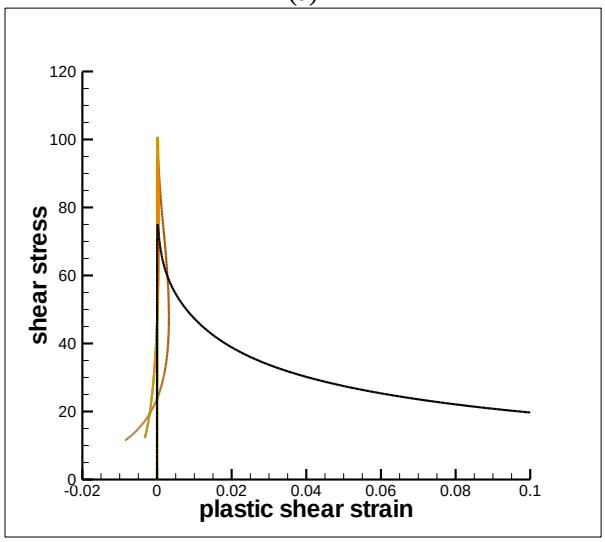

(b)

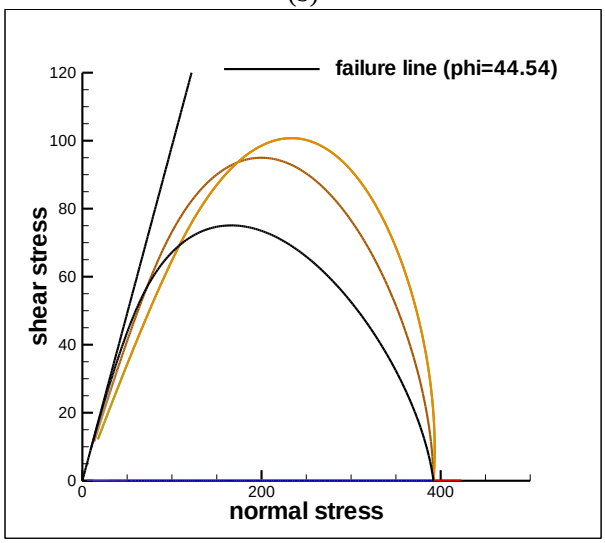

(c)

Figure (4) a) normal stress vs. plastic normal strain b) tangential stress vs. plastic tangential strain c)stress path for sample which has relative density %29.

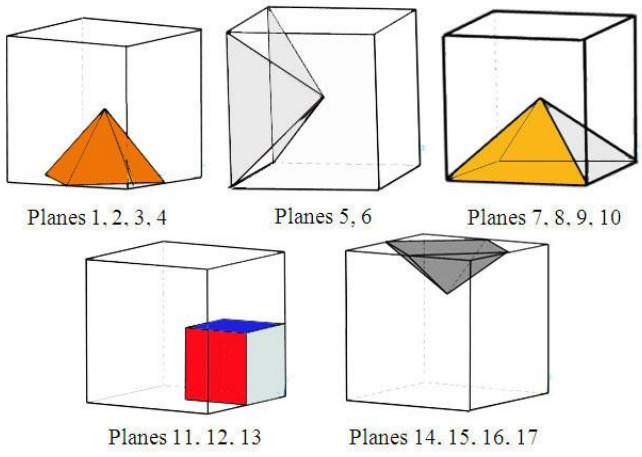

(d)

Figure (4-d) Geometry of the first failed plane is plane number 13 that looses normal stress. It is followed by planes number 1, 2, 3 and 4 followed by planes number 7 and 8 and then plane number 11 decreases normal stress and planes number 14, 15, 16 and 17 are the last set of sheared failed planes.

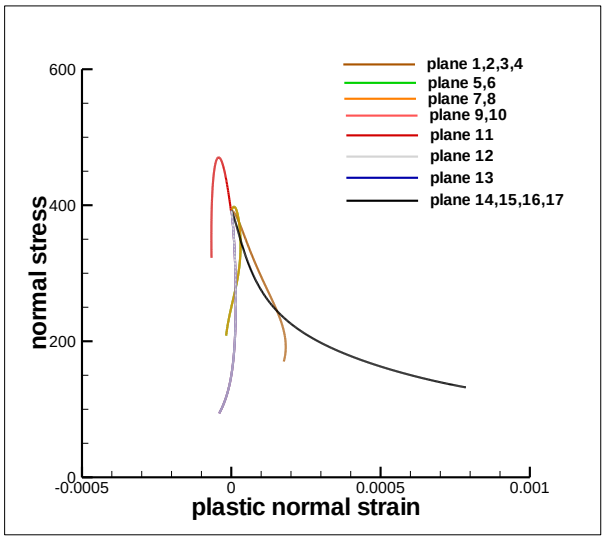

(a)

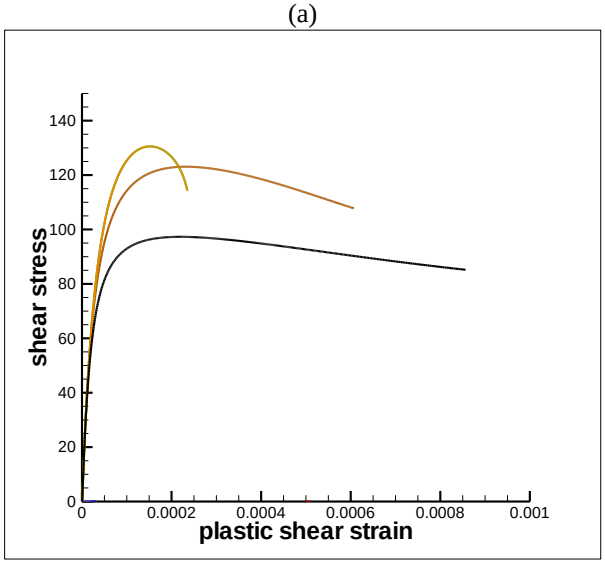

(b)

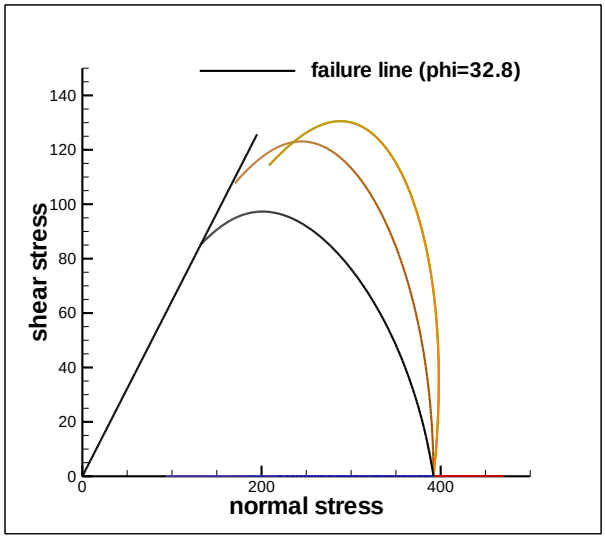

(c)

Figure (5) a) normal stress vs. plastic normal strain b) tangential stress vs. plastic tangential strain c)stress path for sample which has relative density %44.

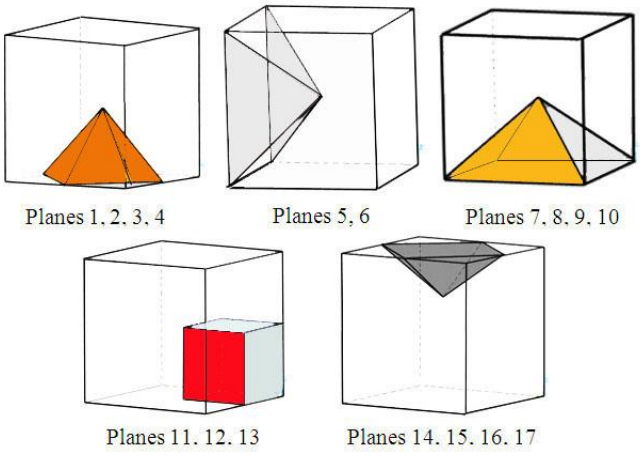

(d)

Figure (5-d) Geometry of the first failed plane is plane number 12 that looses normal stress. It is followed by planes number 14, 15, 16 and 17 followed be planes number 1, 2, 3 and 4, followed by planes number 7 and 8. The normal stress on plane number 11 goes up and comes down.

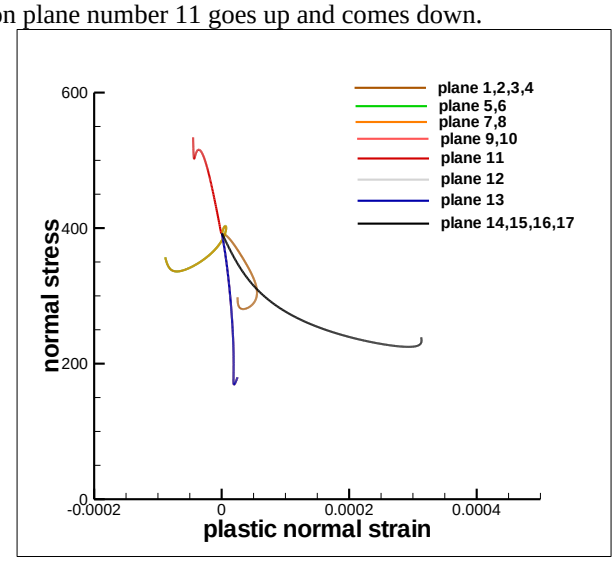

(a)

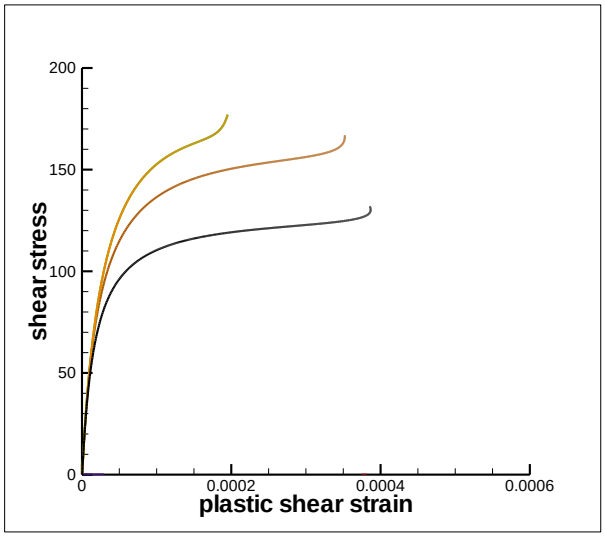

(b)

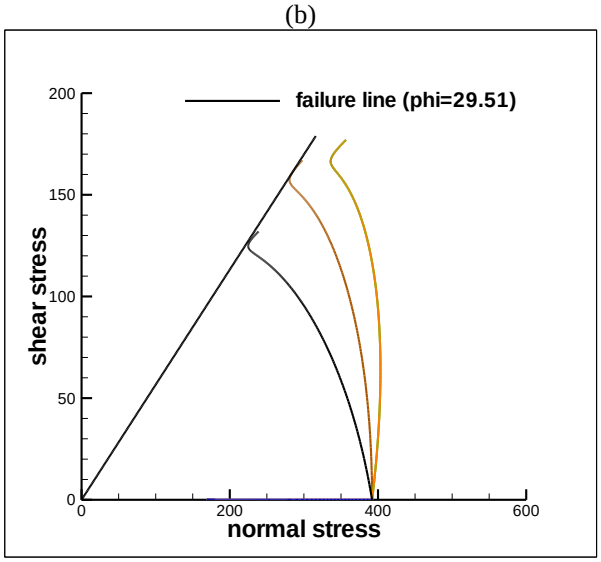

(c)

Figure (6) a) normal stress vs. plastic normal strain b) tangential stress vs. plastic tangential strain c)stress path for sample which has relative density %47.

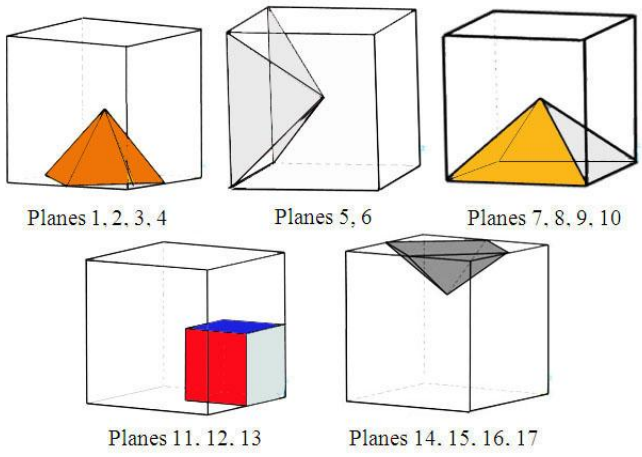

(d)

Figure (6-d) Geometry of the first failed plane loosing normal stress is plane number 13 followed by planes number 14, 15, 16 and 17 followed be planes number 1, 2, 3 and 4 and then planes number 7 and 8, plane number 11 increases normal stress.

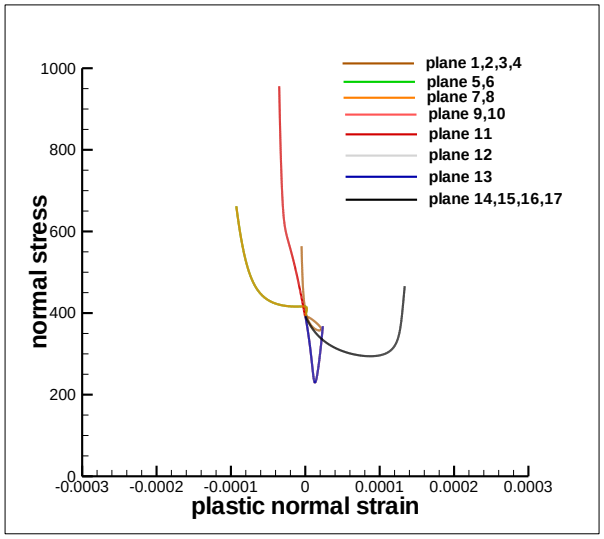

(a)

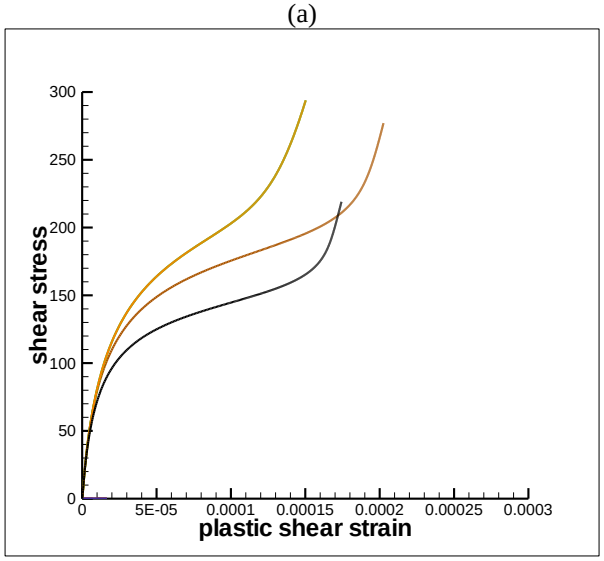

(b)

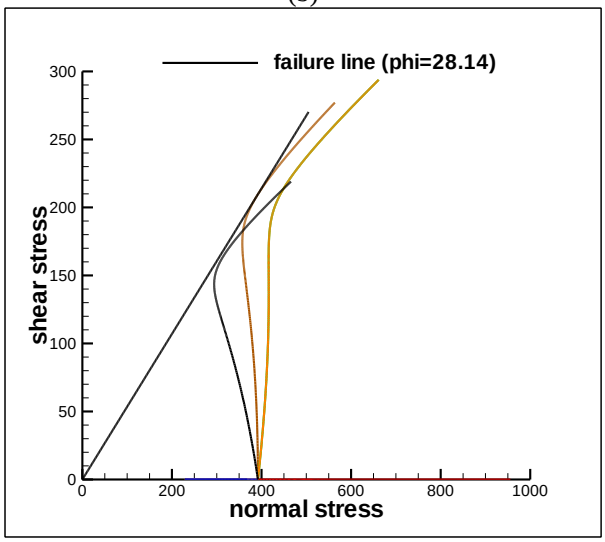

(c)

Figure (7) a) normal stress vs. plastic normal strain b) tangential stress vs. plastic tangential strain c)stress path for sample which has relative density %66.

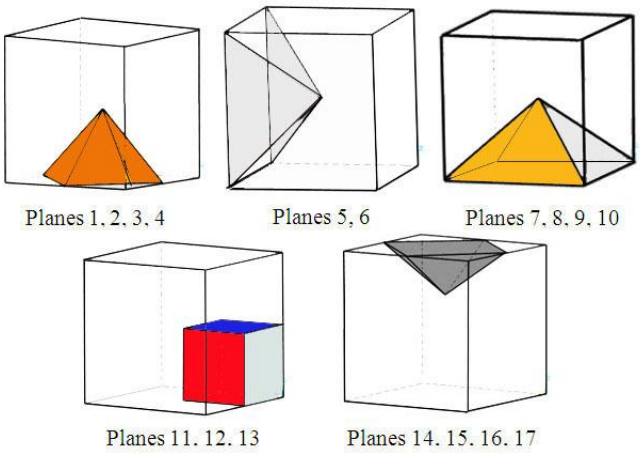

(d)

Figure (7-d) Geometry of the first active plane is number 13 which is followed by (dark) planes number 14, 15, 16 and 17 decreasing and then increasing normal stresses, and the other active planes number 11 followed by planes number 7 and 8 increasing normal stress which are followed by planes number 1, 2, 3 and 4.

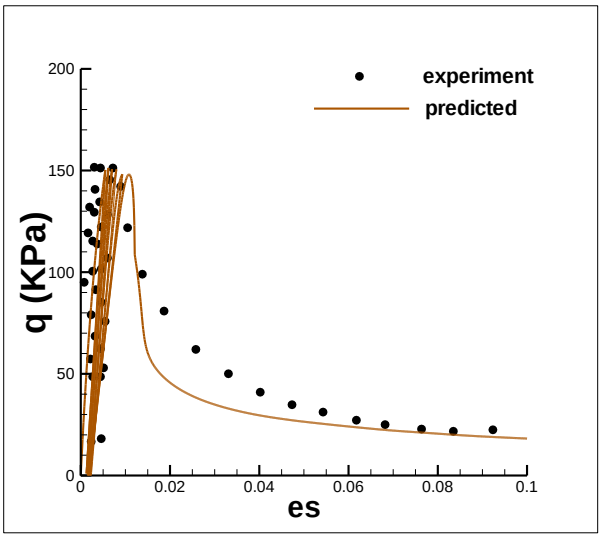

(a)

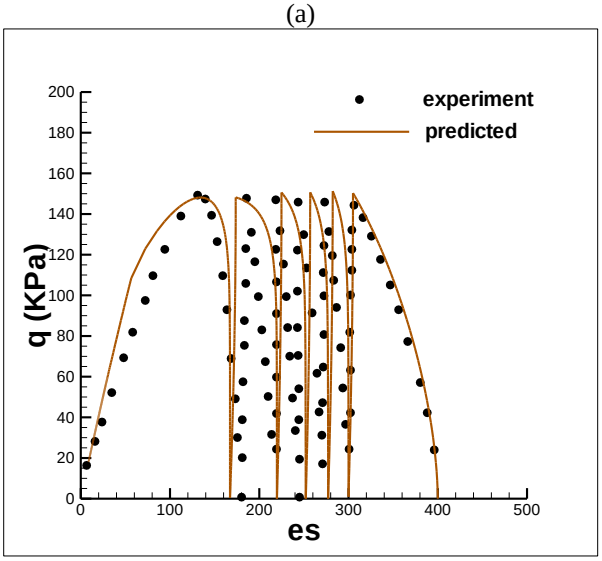

(b)

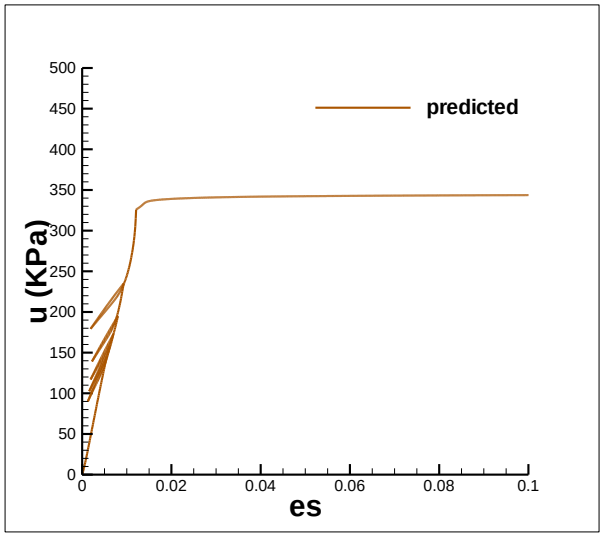

(c)

Figure (8) Undrained behavior of Banding sand (Dr=.29) a) deviatoric stress vs. shear strain b)stress path, c) pore pressure vs. shear strain under cyclic loading (Computed results shown by solid line).

VII. Conclusion

A composition of multi-laminate modulusmatrices is integrated and developed to predict semi-multiscopic behavior of soil including some multi material aspects in engineering. This frame work made such facilities to clarify internal material mechanism during plastic flow and pre-failure internal strain distribution at a point.

A constitutive model for the mechanical behavior of sand under any arbitrary loading conditions was developed using the composition of the theoretical framework of multi-laminate and generalized plasticity approaches. Proposed model can simulate configuration of inside material, pre and final failure mechanism. This novel multi-laminate damage model can simulate behavior of soil specimen under tensile loadings as well as compressive loadings. Moreover, proposed model has excellent features such as capability of seeing induced/inherent anisotropy and also any fabric effects on material behavior, the basis of its formulation is simple, logical and has some physical insights that make it convenient to perceive.

References

1. Batdorf, S.B. and B. Budiansky, 1949. A mathematical theory of plasticity based on the concept of slip. Technical Note 1871, National Advisory Committee for Aeronautics.
2. Carol, I. and Z. Bazant, 1997. Damage and plasticity in multi plane theory. Int. J. Solids & Structures,. 34: 3807-3835.
3. Bazant, Z.P. and P.G. Gambarova, 1984. Crack shear in concrete: Crack band multi plane model. J. Struct. Eng., ASCE, 110: 2015-2036.
4. Pastor, M., Zienkiewicz, O.C., and Chan, A.H.C. (1990), "Generalized plasticity and the modeling of soil behavior", International Journal for Numerical and Analytical Methods in Geomechanics, 14(3), 151-190.
5. Sadrnejad S.A., Multi-laminate elasto-plastic model for granular media, Journal of Engineering, Islamic Republic of Iran, vol.5, Nos.1&2, May 1992-11.
6. Sadrnejad S.A. & PANDE G.N., A Multi-laminate Model For Sand, Proceeding of 3rd International symposium on Numerical Models in Geo-mechanics, NUMOG-III, 8-11 May 1989, Niagara Falls, CANADA.
7. Sadrnejad S.A., Induced Anisotropy Prediction Through Plasticity, Preceding of International Conference on "Engineering Applications of Mechanics", June 9-12, 1992, TEHERAN-IRAN, p.598-605.

8. Sadrnejad S.A., Mathematical approach to Non-associated Plasticity ModulusMatrix for Granular Medium As Continuum, Proceeding of International Conference on "Engineering Applications of Mechanics", June 9-12, 1992, TEHERAN-IRAN, p.343-349.
9. SADRNEZHAD S.A., A MULTI-LAMINATE INDUCED ANISOTROPIC DOUBLE HARDENING ELASTOPLASTIC MODEL FOR SANDS, Journal of Engineering, Islamic Republic of Iran, vol.5, Nos.1&2, May 2001-11.
10. SADRNEZHAD S.A., A CYCLIC QUASI-ELASTIC MODEL FOR LIQUEFACTION OF SATURATED SAND, Journal of Engineering, University of Mashhad, 11th year, no. 1, 1998.
11. SADRNEZHAD S.A., A MULTILAMINATE ELASTOPLASTIC MODEL FOR SEMI SATURATED SOIL, International Journal of Engineering, and Amir-Kabir University of Technology, vol 10, No.40, 1999.
12. SADRNEJAD, S.A., (2006), Fabric Behavior of Sand in post-liquefaction , AMERICAN JOURNAL OF APPLIED SCIENCES, (2005 Science publications), Volume 2, Number 12, 2005 pp 1562-1573.
13. Sadrnejad, S.A., Karimpour, H., Drained and Undrained Sand Behaviour by Multilaminate Bounding Surface Model, International Journal of Civil Engineering, vol.9, No.2, 2011.